Int J Clin Exp Med 2015;8(7):10501-10507
www.ijcem.com /ISSN:1940-5901/IJCEM0008309

Original Article

Promising potency of retinoic acid-poly(ethylene glycol)-thiol gold nanoparticle conjugates for cervical cancer treatment

Li Ye, Qian Song

Department of Obstetrics and Gynecology, Taizhou Cancer Hospital, Taizhou 317502, Zhejiang, China

Received March 22, 2015; Accepted June 30, 2015; Epub July 15, 2015; Published July 30, 2015

Abstract: We investigated the effect of synthesized retinoic acid-poly(ethylene glycol)-thiol gold nanoparticle conjugates on cervical carcinoma cells. Cervical cancer is the major cause of deaths for the women of reproductive age in the developing countries. Compared to retinoic acid, the nanoparticle conjugates exhibited better activity against cervical carcinoma. Selective delivery of gold nanoparticle conjugates to estrogen receptor positive cervical cancer cells with 6-fold enhanced drug potency was observed. Transfer of gold nanoparticles was found to be dominated by estrogen ligand and receptor. It appeared that retinoic acid nanoparticle conjugates were selectively taken and retained by the estrogen receptor alpha present in the plasma membrane. Thus IC_{50} values for RA-PEG-SH were significantly improvedon nanoparticle ligation. Cells on treatment with RA-PEG-SH-AuNPsshowed growth inhibition at 12 and 24 h after incubation. The IC_{50} for RA in RA-PEG-SH-AuNPs after 12 and 24 h were 3 and 1 μM, respectively. Thus, the use of RA nanoparticle conjugates can be a better strategy for cervical carcinoma treatment.

Keywords: Cervical carcinoma, nanoparticle, endocytosis, estrogen receptor, retinoic acid

Introduction

The second leading cause of cancer deaths in women throughout the world is cervical cancer. It is estimated that around 500,000 new cases of cervical cancer are diagnosed globally every year. The HPV3 infected women show multistage process of carcinogenesis that develops and progresses into cervical cancer [1]. Initially a precursor lesion appears which progress to invasive cancer [2]. However, in cervical carcinogenesis the premalignant phase usually lasts for 5-10 years, making it suitable for chemopreventive therapy.

Retinoic acid has been shown to be very effective against various types of cancers including ovarian adenocarcinoma, head and neck cancer, breast cancer, human malignant gliomas and acute promyelocyticleukemia [3-7]. Additionally, cell cycle behaviour is also influenced by all-trans retinoic acid [8, 9]. Despite the promising activity of retinoic acid in the treatment of cancers, low aqueous solubility is a great challenge for its clinical applications [10, 11]. To overcome the drawback, polymeric micelles like glycol chitosan micelles have been developed [12]. RA-incorporated GC nanoparticles inhibited the proliferation of HuCC-T1 cholangiocarcinoma cells at higher than 20 μg/mL of RA concentration [13]. In the present study, the retinoic acid nanoparticle conjugates were synthesized with an aim to overcome the limitation of solubility and enhance selective intracellular delivery. This technique enhanced the potency and selective intracellular delivery of RA-targeted gold nanoparticles to ER(+) cervical cancer cells. The uptake of particles was found to be dependent both on receptor as well as ligand and lead to a 3.5-fold enhanced drug potency compared to the free drug.

In the current study, a PEG-SH-RA derivative was synthesized and subsequently subjected to gold nanoparticle (AuNP) conjugation (**Figure 1**). This technique enhanced the potency and selective intracellular delivery of RA-targeted gold nanoparticles to ER(+) cervical cancer cells.

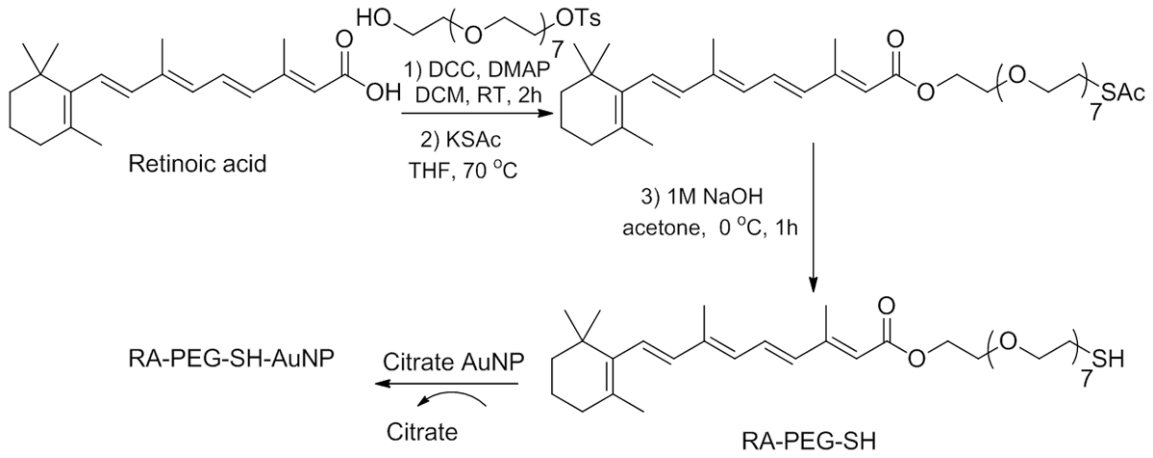

Figure 1. Synthesis of retinoic acid-poly(ethylene glycol)-thiol gold nanoparticle conjugates.

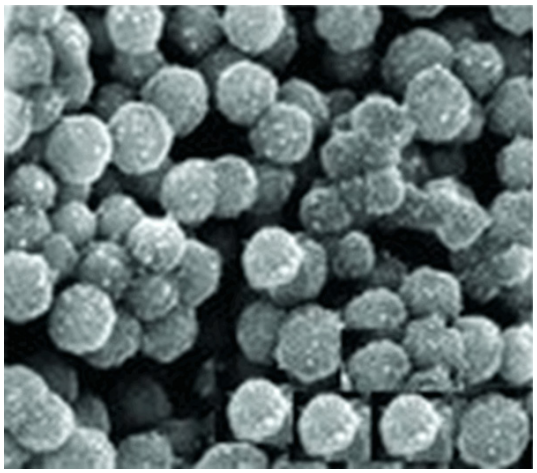

Figure 2. Formation of the nanoparticle conjugates.

Nanoparticles with their multivalent nature of surfaces have been shown to be very effective for the purpose of diagnosis and treatment [14-18]. There is an increase in binding affinity in proportion to the density of binding sites after nanoparticle conjugate are formed. The uptake of nanoparticle conjugates greatly enhances delivery rates in the cases where intracellular drug transport relies on passive diffusion [19, 20]. It is reported that enhanced permeability and retention which are responsible for preferential accumulation at tumor sites in vivo is associated with nano-size of the drug conjugates [21, 22]. The properties of nanoparticles including biocompatibility [23, 24], stability [25], and potential use in phothermal laser treatments proved them to be excellent candidates for cancer treatment strategies [21, 25-29].

Materials and methods

Reagents and chemicals

Octa(ethylene glycol) (OEG), retinoic acid, and other chemicals were purchased from Sigma Chem. Co. Ltd. (St. Louis, MO, USA).

Synthesis of gold nanoparticles and their conjugation

We subjected retinoic acid to esterification using DCC and DMAP. The retinoic acid ester was treated with thioacetate followed by deprotection to result conjugate nanoparticle. The chloroauric acid after Turkevich reduction was used for the synthesis of gold nanoparticles. The 100 mL of 1.0 mM aqueous $HAuCl_4$ solution was refluxed and to it 10 mL of 3.5 mg/mL aqueous sodium citrate was added while stirring. Heating was stopped after half an hour and stirring was continued for 45 minutes. The solution containing crude AuNP was subjected to centrifugation at 12, 000 × *g*. Five milligram of RA-PEG-SH suspended in 100 μL of ethanol was diluted to 0.5 mM solution by distilled water. To the AuNPs, 1:1 mixture of RA-PEG-SH and PEG-SH was added and the mixture was sonicated overnight. The concentration of citrate-capped gold nanosphere was estimated by molar extinction coefficient.

Characterization of gold nanoparticle bioconjugation

The synthesized gold nanoparticles were characterised by diffraction-contrast transmission electron microscopy (TEM, JEOL 100CX II) and

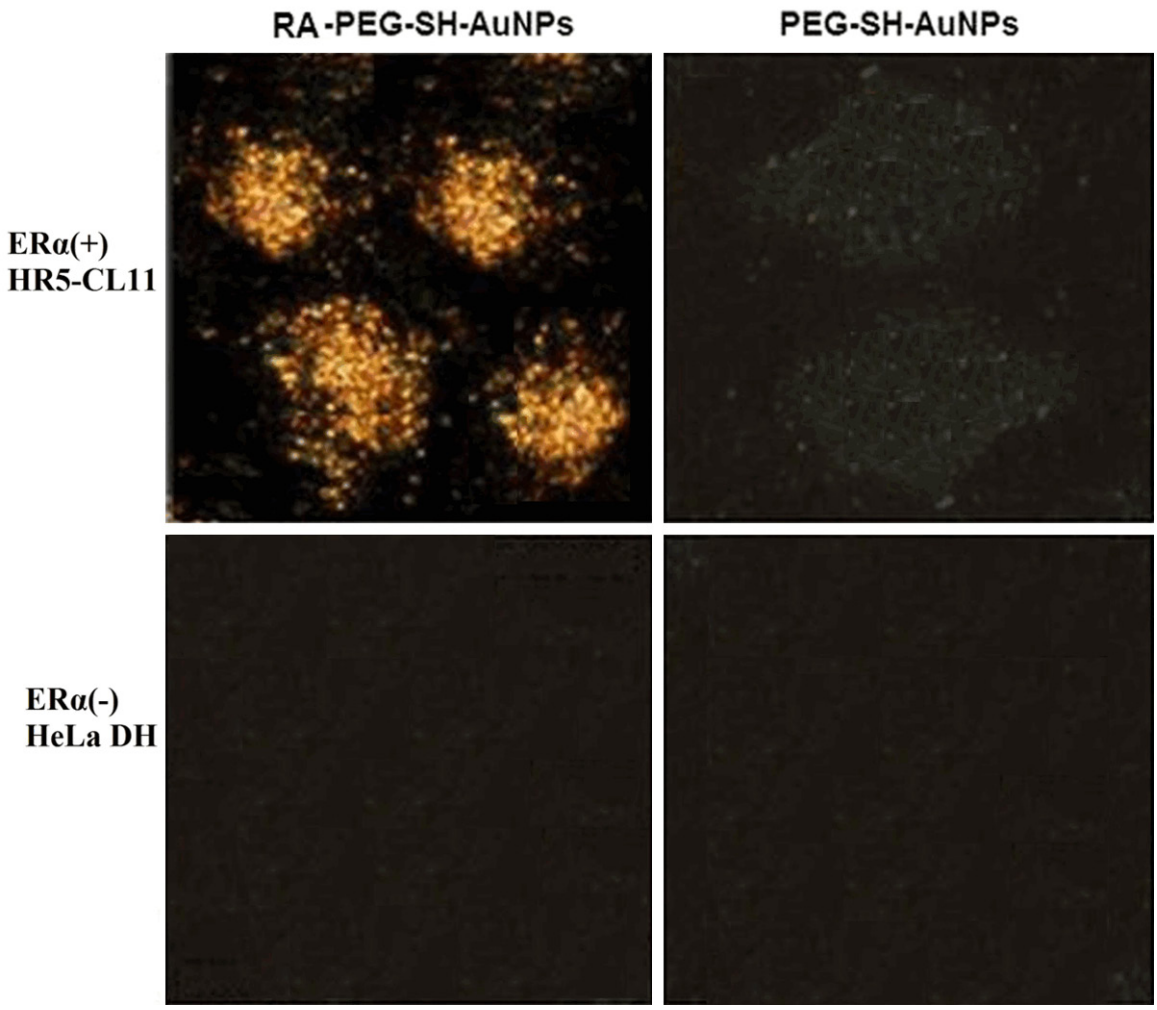

Figure 3. Dark-field scattering microscopy showing ligand-and receptor-dependent intracellular targeting of cervical cancer cells by gold nanoparticle conjugates. Representative dark-field scattering images of ERα(+)HR5-CL11 or ERα(-)HeLa DH human cervical cancer cells incubated for 24 h with 10 μM RA-PEG-SHAuNP and PEG-SH-AuNP conjugates.

UV-Vis absorption spectroscopy (Ocean Optics, HR4000CGUV-NIR) techniques. Absorption was measured at 280 nm to determine the number of RA-PEG-SH ligands per nanoparticle. The Zeta potential of the gold nanoparticles and conjugates was determined by NanoZSZ-etasizer particle analyzer (Malvern) equipped with a 633 nm laser.

Cell culture and nanoparticle incubation

Erα(-)HeLa DH and Erα(+)HR5-CL11 cervical cancer cells or ERα(+) (CaSki) cells were purchased from Sigma-Aldrich. The cells were cultured in DMEM growth media at 37°C in humidified atmosphere containing 5% CO_2. The medium was changed by the media containing gold nanoparticle conjugates.

Cell viability assay

In MTT assay, ERα(-)HeLa DH and ERα(+)HR5-CL11 cervical cancer cells grown for 24 h in a medium containing gold nanoparticle conjugates. The cells were then washed twice with sterile Dulbecco's phosphate-buffered saline (DPBS). The activity of mitochondrial dehydrogenase was then examined using 3-(4,5-dimethylthiazol-2-yl)-2,5-diphenyltetrazolium bromide (MTT). The activity was determined using statistical analysis *t* test and SpectraMax Plus 384 microplate reader.

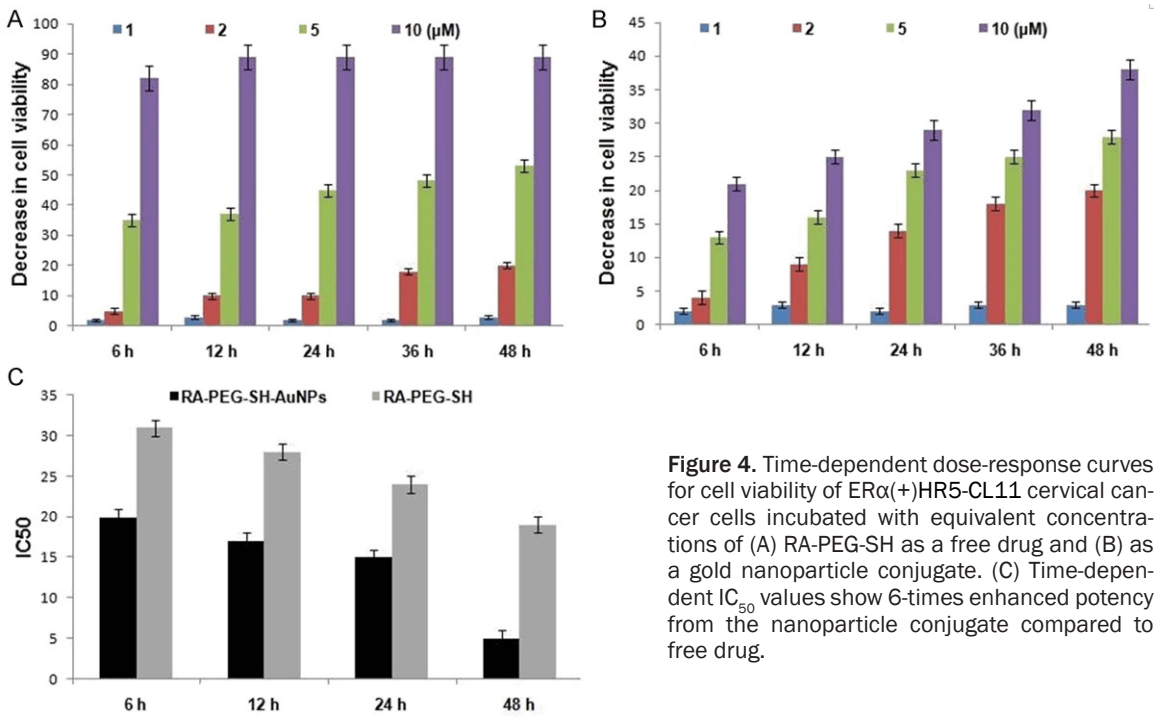

Figure 4. Time-dependent dose-response curves for cell viability of ERα(+)HR5-CL11 cervical cancer cells incubated with equivalent concentrations of (A) RA-PEG-SH as a free drug and (B) as a gold nanoparticle conjugate. (C) Time-dependent IC_{50} values show 6-times enhanced potency from the nanoparticle conjugate compared to free drug.

Absorption microspectrometry and dark-field scattering microscopy

The sterilized cover slips were put in 0.3 μm filtered 0.05 mg/mL collagen (Roche) solution for 6 h. The coated surfaces were washed with sterile PBS and placed in 12-well plates. Incubation of the substrates with nanoparticle conjugates was followed by washing with sterile DPBS buffer. For fixing of the cells cold 10% paraformaldehyde was used. The coverslips coated with glycerol were mounted and sealed onto glass slides. The inverted objective Olympus IX70 microscope fitted with a dark-field condenser (U-DCW) was used for dark-field microscopy. The optical extinction spectra were recorded on SEE110 absorption microspectrometer.

Results

Formation of the RA-PEG-SH-AuNPs conjugate

The absorbance for RA and its conjugates was measured at 280 nm. Comparison of the absorbance before conjugation to nanoparticles and after removal indicated that 15000 RA-PEG-SH ligands are bound to each nanoparticle. Binding of 15000 ligands accounts for around 51% of the theoretical surface coverage for a 25 nm diameter Au(111) surface. A significant change was observed in the zeta potential from -38.4 to -5.79 mV on RA-PEG-SH functionalization. The findings clearly suggested the formation of RA-PEG-SH-AuNPs conjugate (**Figure 2**).

Nanoparticle uptake by the cervical carcinoma cells

ERα(-)HeLa DH and ERα(+)HR5-CL11 cervical cancer cells were incubated with 10 μM RA-PEG-SH-AuNPs and PEG-SH-AuNPs for a period of 24 h. The intracellular uptake of nanoparticles was analysed by dark-field scattering microscopy. On examination, we observed a higher level of intracellular and perinuclear RA-PEG-SH-AuNPs localization in ERα(+)HR5-CL11cervical cancer. In Erα(-)HeLa DH cells RA-PEG-SH-AuNPs localization was found to absent (**Figure 3**).

Neither Erα(+)HR5-CL11 nor Erα(-)HeLa DH was observed to show uptake of AuNPs labelled only with PEG-SH. We also found that the uptake of RA-PEG-SH-AuNPs by Erα(+)HR5-CL11 cells was dependent on the time. Incubation of the cells with RA-PEG-SH-AuNPs for 6 h showed labelling only in the marginal cell surface. The labelling was visible in the perinuclear and cytoplasmic locations after 24 h. For determination of the relation between expression of ER and gold particle targeting incubation of the ERα(+) human carcinoma cells (CaSki) was performed in the presence of 10 μM RA-PEGSH-

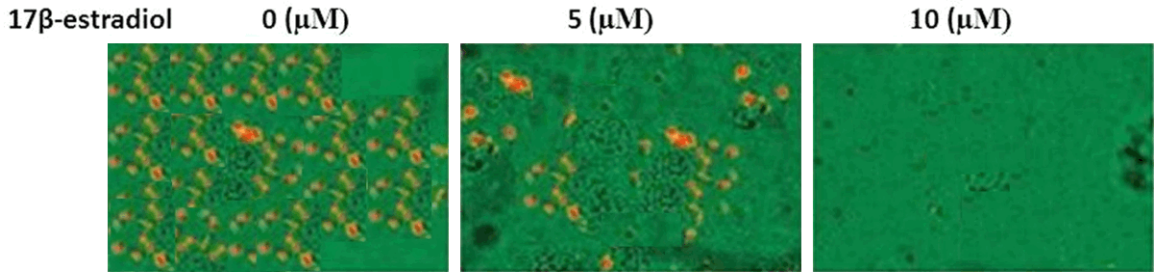

Figure 5. Representative dark-field scattering (red) and bright-field transmission (green) image overlays of RA-PEG-SH-AuNP competitive binding following 24 h incubation with 17*β*-estradiol. ERα(+) cervical cancer cells (CaSki) were incubated overnight with increasing concentrations of estrogen, followed by 24 h incubation with 5 *μ*M RA-gold nanoparticle conjugates.

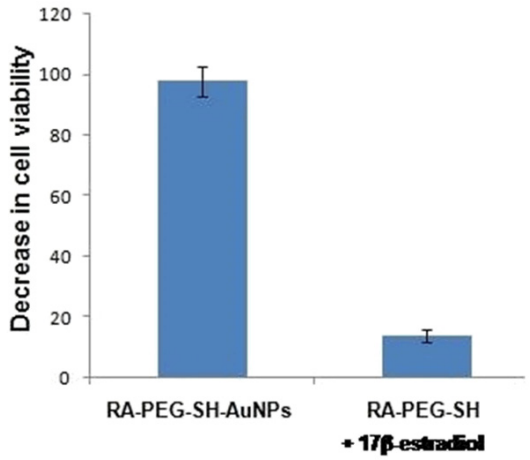

Figure 6. Suppression of RA-PEG-SH-AuNP activity by estrogen competition in ERα(+) cervical cancer cells. Growth inhibition of cells incubated for 24 h with 10 *μ*M RA-PEG-SH-AuNPs when previously untreated and treated overnight with 10 *μ*M 17*β*-estradiol.

AuNPs and PEG-SH-AuNPs for 24 h. CaSki cells were found to selectively uptake RA-PEGSH-AuNPs.

Effect of RA-PEG-SH-AuNPs on AuNP surface plasmon extinction

Incubation of the ERα(+) and ERα(-) cervical cells with RA-PEG-SH-AuNPs resulted in the AuNP surface plasmon extinction exclusively from perinuclear regions of ERα(+) cells. However, no such effect was observed in the cells incubated with PEG-SH-AuNPs.

Effect of RA-PEG-SH-AuNPs on cervical cell viability

The ERα(+)HR5-CL11 cervical cancer cells were incubated with similar doses of RA-PEG-SH (free drug) and the nanoparticle conjugate. We observed a time time-dependent dose-response curves (**Figure 4A**, **4B**). Comparison of the IC_{50} values for free drug and its AuNP conjugate showed 6-fold enhanced potency for RA-PEGSH-AuNPs (**Figure 3C**). Thus IC_{50} values for RA-PEG-SH were markedly improved on nanoparticle ligation. Cells on treatment with RA-PEG-SH-AuNPs showed growth inhibition at 12 and 24 h after incubation. The IC_{50} for RA in RA-PEG-SH-AuNPs after 12 and 24 h were 3 and 1 *μ*M, respectively.

Effect of estrogen nanoparticle uptake by the cervical carcinoma cells

Incubation of the ERα(+)CaSki cervical cells with various doses of estrogen, an ERR's endogenous ligand 17β-estradiol was followed by incubation for 24 h with 5 *μ*M RA-PEGSH-AuNPs. We observed inhibition of RA-PEG-SH-AuNP intracellular localization at estrogen concentrations as low as 20 nM (**Figure 5**). Decreased cell surface labelling was also observed with increasing estrogen concentration. This suggests that a greater ERα binding affinity for 17β-estradiol compared to that of RA.

ERα(+) cervical cells were incubated for 24 h with 10 *μ*M RA-PEG-SH-AuNPs after blocking for 12 h with equimolar concentrations of estrogen was performed (**Figure 6**). The cells treated initially with estrogen showed inhibition of cytotoxic activity of RA-labelled AuNPs. However, in the absence of estrogen the effect of RA-labelled AuNPs was maintained. These findings correlate ERR binding with both RA-PEG-SH-AuNP intracellular localization and subsequent cell death.

Discussion

We observed that retinoic acid-poly(ethylene glycol)-thiol gold nanoparticle conjugates selectively targeted estrogen receptor alpha in human cervical cancer cells. The efficiency of the nanoparticle conjugates was about 6-times enhanced compared to free drug. The Optical microscopy and spectroscopy showed higher degree of perinuclear and cytoplasmic localization of the targeted particles. However, we did not observe any localization or cytotoxic effect from the untargeted nanoparticles. Time-dependent dose-response studies showed that increased potency results from increased rates of drug transport by nanoparticle uptake versus passive diffusion of the free drug. Receptor-selective and estrogen-competitive cytotoxicity and uptake of the nanoparticle conjugates indicates no additive effects associated with the gold particles themselves. The plasma membrane localized ERα may facilitate selective endocytotic transport of these therapeutic nanoparticle conjugates. The lack of significant growth inhibition by the free drug at short incubation times, together with an observed decrease in the disparity between IC_{50} values of the free drug and the AuNP conjugate over time, and obvious ligand-dependent response indicate increased rates of RA-PEG-SH transport by the AuNP conjugate.

The ERα expression-dependent nanoparticle uptake observed suggests that the cell membrane-associated receptor may facilitate intracellular nanoparticle transport. Indeed, plasma membrane localized ERα has been shown both as antibody epitopes for the nuclear receptor and 17β-estradiol in mammalian cells [30, 31]. It is reported that intracellular transport and caveolar localization of ERα lies in the plasma membrane [32]. The role of plasma membrane localized ERα in contributing to receptor-mediated endocytosis of RA-PEG-SH-AuNP conjugates was proved. The cell viability was shown to increase by 87% following incubation with 10 μM RA-PEG-SHAuNPs for 6 h at 4°C. This indicated that endocytosis, in addition to ERα binding and intracellular particle delivery, is required for therapeutic response from RA labelled AuNP conjugates.

Conclusions

Thus retinoic acid nanoparticle conjugate is an effective strategy for the cervical cancer therapy.

Disclosure of conflict of interest

None.

Address correspondence to: Li Ye, Department of Obstetrics and Gynecology, Taizhou Cancer Hospital, No. 1 Zhenxing Road, Xinhe Town, Taizhou 317502, Zhejiang, China. Tel: 0086-576-8659004; Fax: 0086-576-86590042; E-mail: yeli43434@gmail.com

References

[1] Schoell WM, Janicek MF, Mirhashemi R. Epidemiology and biology of cervical cancer. Semin Surg Oncol 1999; 16: 203-211.

[2] Smith WL, Garavito RM, DeWitt DL. Prostaglandin endoperoxide H synthases (cyclooxygenases)-1 and -2. J Biol Chem 1996; 271: 33157-33160.

[3] Huang EJ, Ye YC, Chen SR, Chai JR, Lu JX, Zhoa L, Gu LJ, Wang ZY. Use of all-trans retinoic acid in the treatment of acute promyelocyticleukemia. Blood 1988; 72: 567-572.

[4] Lehman PA, Slattery JT, Franz TJ. Percutaneous absorption of retinoids: influence of vehicle, light exposure, and dose. J Invest Dermatol 1988; 91: 56-61.

[5] Szuts EZ, Harosi FI. Solubility of retinoids in water. Arch Biochem Biophys 1991; 287: 297-304.

[6] Jeong YI, Kim SH, Jung TY, Kim IY, Kang SS, Jin YH, Ryu HH, Sun HS, Jin S, Kim KK, Ahn KY, Jung S. Polyion complex micelles composed of all-trans retinoic acid and poly (ethylene glycol)-grafted chitosan. J Pharm Sci 2006; 95: 2348-60.

[7] Chung KD, Jeong YI, Chung CW, Kim do H, Kang DH. Anti-tumor activity of all-trans retinoic acid-incorporated glycol chitosan nanoparticles against HuCC-T1 human cholangiocarcinoma cells. Int J Pharmaceutics 2012; 422: 454-461.

[8] Krupitza G, Hulla W, Harant H, Dittrich E, Kallay E, Huber H. Retinoic acid induced death of ovarian carcinoma cells correlates with c-myc stimulation. Int J Cancer 1995; 61: 649-659.

[9] Defer GL, Adle-Biassette H, Ricolfi F, Martin L, Authier FJ, Chomienne C, Degos L, Degos J. All-trans retinoic acid in relapsing malignant gliomas: clinical and radiological stabilization associated with the appearance of intratumoral calcifications. J Neurooncol 1997; 34: 169-177.

[10] Crocetti E, Trama A, Stiller C, Caldarella A, Soffietti R, Jaal J, Weber DC, Ricardi U, Slowinski J, Brandes A; RARECARE working group. Epidemiology of glial and non-glial brain tumors in Europe. Eur J Cancer 2012; 48: 1532-42.

[11] Tanaka S, Louis DN, Curry WT, Batchelor TT, Dietrich J. Diagnostic and therapeutic avenues for glioblastoma: no longer a dead end? Nat Rev Clin Oncol 2013; 10: 14-26.
[12] Stummer W, Kamp MA. The importance of surgical resection in malignant glioma. Curr Opin Neurol 2009; 22: 645-649.
[13] Norden AD, Wen PY. Glioma therapy in adults. Neurologist 2006; 12: 279-292.
[14] Weissleder R, Kelly K, Sun EY, Shtatland T, Josephson L. Cell-specific targeting of nanoparticles by multivalent attachment of small molecules. Nat Biotechnol 2005; 23: 1418-1423.
[15] Montet X, Funovics M, Montet-Abou K, Weissleder R, Josephson L. Multivalent effects of RGD peptides obtained by nanoparticle display. J Med Chem 2006; 49: 6087-6093.
[16] Gestwicki JE, Cairo CW, Strong LE, Oetjen KA, Kiessling LL. Influencing receptor-ligand binding mechanisms with multivalent ligand architecture. J Am ChemSoc 2002; 124: 14922-14933.
[17] Goodman CM, Rotello VM. Biomacromolecule surface recognition using nanoparticles. Mini Rev Org Chem 2004; 1: 103-114.
[18] Gibson JD, Khanal BP, Zubarev ER. Paclitaxel-functionalized gold nanoparticles. J Am Chem Soc 2007; 129: 11653-11661.
[19] Cho K, Wang X, Nie S, Chen Z, Shin DM. Therapeutic nanoparticles for drug delivery in cancer. Clin Cancer Res 2008; 14: 1310-1316.
[20] Chawla JS, Amiji MM. Biodegradable poly([var epsilon]-caprolactone) nanoparticles for tumor-targeted delivery of tamoxifen. Int J Pharm 2002; 249: 127-138.
[21] Maeda H. The enhanced permeability and retention (EPR) effect in tumor vasculature: The key role of tumor selective macromolecular drug targeting. AdV Enzyme Regul 2001; 41: 189-207.
[22] von Maltzahn G, Park JH, Agrawal A, Bandaru NK, Das SK, Sailor MJ, Bhatia SN. Computationally guided photothermaltumor therapy using long-circulating gold nanorod antennas. Cancer Res 2009; 69: 3892-3900.
[23] Khan JA, Pillai B, DasTK, Singh Y, Maiti S. Molecular effects of uptake of gold nanoparticles in HeLa cells. Chem Bio Chem 2007; 8: 1237-1240.
[24] Zhang F, Skoda MWA, Jacobs RMJ, Zorn S, MartinRA, Martin CM, Clark GF, Goerigk G, Schreiber F. Gold nanoparticles decorated with oligo(ethylene glycol) thiols: Protein resistance and colloidal stability. J Phys Chem A 2007; 111: 12229-12237.
[25] Dickerson EB, Dreaden EC, Huang X, El-Sayed IH, Chu H, Pushpanketh S, McDonald JF, El-Sayed MA. Gold nanorod assisted near-infrared plasmonicphotothermal therapy (PPTT) of squamous cell carcinoma in mice. Cancer Lett 2008; 269: 57-66.
[26] O'Neal DP, Hirsch LR, Halas NJ, Payne JD, West JL. Photothermaltumor ablation in mice using near infrared absorbing nanoshells. Cancer Lett 2004; 209: 171-176.
[27] Huang X, El-Sayed IH, El-Sayed MA. Cancer cell imaging and photothermal therapy in the near-infrared region by using gold nanorods. J Am Chem Soc 2006; 128: 2115-2120.
[28] Huff TB, Tong L, Zhao Y, Hansen MN, Cheng JX, Wei A. Hyperthermic effects of gold nanorods on tumor cells. Nanomedicine 2007; 2: 125-132.
[29] Hirsch LR, Stafford RJ, Bankson JA, Sershen SR, Rivera B, Price RE, Hazle JD, Halas NJ, West JL. Nanoshell-mediated near-infrared thermal therapy of tumors under magnetic resonance guidance. Proc Natl Acad Sci U S A 2003; 100: 13549-13554.
[30] Levin ER. Integration of the extranuclear and nuclear actions of estrogen. Mol Endocrinol 2005; 19: 1951-1959.
[31] Zivadinovic D, Gametchu B, Watson CS. Membrane estrogen receptor-alpha levels in MCF-7 breast cancer cells predictcAMP and proliferation responses. Breast Cancer Res 2005; 7: R101-R112.
[32] Razandi M, Oh P, Pedram A, Schnitzer J, Levin ER. ERs associate with and regulate the production of caveolin: Implications for signaling and cellular actions. Mol Endocrinol 2002; 16: 100-115.